Unique Catalytic Activity of Mesoporous Catalysts in Friedel-Crafts Benzylation of Benzene

Ahmed Arafat and Yahia Alhamed

Chemical & Materials Engineering Department
Faculty of Engineering, King Abdulaziz University
Jeddah 21589 P.O. Box 80204, Saudi Arabia, akhamis@kau.edu.sa

Abstract

Different samples of metal-incorporated MCM-41 were prepared and used as catalysts in Friedel-Craft's benzylation of benzene. The catalytic performance was evaluated by off-line GC analysis. Fe-MCM-41 exhibited excellent activity, the sample with Si/Fe ratio = 10 showed 92% conversion with 95% selectivity towards diphenylmethane within a few minutes. Generally, the activity per Fe-site was an order of magnitude higher for the samples containing a combination of Fe_2O_3 nano-particles and isolated Fe^{3+} sites. A synergy of two catalytic centers (particles and isolated sites) is proposed to explain the high performance of the highly loaded samples. The catalytic performance of Fe-MCM-41 was superior to other metal-containing MCM-41 (e.g. Ga, Sn, and Ti) catalysts, or other Fe-containing mesoporous materials (e.g. Fe-HMS).

Introduction

The electrophilic substitution reaction of alkyl groups in an aromatic system are known since 1877. Friedel-Crafts type reactions are considered as one of the most important reactions in organic synthesis. Benzylation of benzene using benzyl chloride to afford diphenylmethane is an interesting example as substitute for polychlorobenzene in the application of dielectrics.
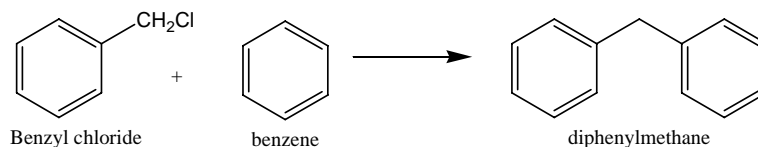
Although, homogeneous, Lewis or Brønsted acids were commonly used as catalysts in Friedel-Crafts type reactions [1] they create several problems such as polyalkylations and rearrangements which are difficult to avoid, in addition to corrosion, toxicity, and catalyst recovery. An important step forward to phase put these problems is the application of solid acid catalysts in these reactions.

A number of solid catalysts have been evaluated. Clark et al.[2,3] reported montmorillonite-supported zinc (Clayzinc) and nickel chloride as highly active for catalyzing Friedel-Crafts alkylations. Another approach was clays [4,5]. Choudary found that iron pillared clays (FePILCs) were efficient catalysts, producing quantitative conversions with greatly reduced amounts of catalysts and shorter reaction times [6]. However, FePILCs were quite labile even under ambient conditions[7]. Aging the materials for periods of 3 months at $25^{o}C$ resulted in a loss of the 011 ordering, redistribution of iron and a concomitant change in the degree of polycation polymerization. At the same time, the poor thermal stability of clay materials gives rise to difficulties in regeneration. Heteropolyacid salts[7-9] and zeolites (e.g. HY [10], and H-β[11]) were also used as catalysts for Friedel-Crafts reactions. It is interesting to mention that, in spite of its very strong acidity, zeolite H-ZSM-5 shows little or no activity in the

benzylation of benzene [10]. On the other hand, Fe-ZSM-5 was also reported[12] and its catalytic activity was better than that of clays, however, the reaction was slow.

The use of metal-containing mesoporous materials as catalysts has also been reported[13,14]. Their activities, although better, still did not lead to complete conversions over a period of four hours or so. In the case of Fe-HMS the one-dimensional pore structure might introduce less than optimal diffusion to and from the active centers. The nature of the active sites might also be an issue, as completely isolated iron atoms may not be the most favourable sites. Indeed, nano-sized Fe_2O_3 clusters could be proven to be more reactive due to their high degree of coordinative unsaturation.

In this work, the catalytic performance of M-MCM-41 (M=Fe, Ga, Sn and Ti) was evaluated in the liquid phase Friedel-Crafts benzylation of benzene. The effects of metal loading and reaction temperature were evaluated. Moreover, a reaction mechanism based on a kinetic study is given as well.

Experimental

Preparation and Characterization of Catalysts

Fe-MCM-41 samples with 4 different Si/Fe ratio of (100, 50, 20 and 10) were used for this study. MCM-41 materials were synthesized applying a modified Stöber's synthesis of monodisperse silica spheres [15]. Typically, 2.5 g of n-hexadecyltrimetilammonium bromide (C_{16}TMABr, Aldrich) was dissolved in 46.3 g of de-ionized water and mixed with 60 g of absolute ethanol. To this clear solution 16.9 g of aqueous ammonia solution (25 m/m %) was added while stirring. Stirring was continued for another 15 min. This followed by addition of 4.7 g of tetraethylorthosilicate (TEOS, Aldrich 98%). The resulting hydrogel having the molar composition of 1 TEOS : 0.3 C_{16}TMABr : 11 NH_3 : 144 H_2O : 58 EtOH was stirred for 2 h and aged for additional 16 h at room temperature. Template removal was carried out by calcinations of samples under nitrogen up to 773 K at a heating rate of 2 K/min, followed by isothermal treatment at the same temperature for 2 h in air.

Fe-MCM-41 samples with various iron contents were prepared by slightly modifying the original procedure in order to avoid the precipitation of iron-hydroxides in the strongly alkaline medium. C_{16}TMABr, water, ethanol and TEOS were mixed in the desired proportion. To this solution 0.46 or 0.18 g of $Fe(NO_3)_3 \cdot 9H_2O$ (Si/Fe = 20 and Si/Fe = 50, respectively, Fluka) was added and stirred for 30 min resulting in a light yellow, clear solution. The required amount of ammonia was poured into this solution at one time causing immediate gel precipitation. The color of the precipitate was pale beige. Calcination was carried out at 790K with the same procedure as described above.

Catalyst Characterization.

XRD patterns were recorded using Cu Kα radiation (l = 1541 nm) on a Philips PW 1840 diffractometer equipped with a graphite monochromator. The samples were scanned over the range of 0.1–80° 2θ with steps of 0.02^o.

Nitrogen sorption isotherms were recorded on a Quantachrome Autosorb-6B at 77 K. Mesoporosity was calculated from the adsorption branch using the Barret–Joyner–Halaenda (BJH) model.

Diffuse reflectance UV–vis spectra were recorded on a CaryWin 300 spectrometer under atmospheric conditions using $BaSO_4$ as reference. Samples were scanned from 190 to 800 nm.

The UV-Vis absorption data were converted to Kubelka-Munk units using the following formula:

$$F(R) = \frac{(1-R)^2}{2R}$$

Elemental analysis was carried out by using instrumental neutron activation analysis (INAA)[16] on a THER nuclear reactor with a thermal power of 2.0 MW and a maximum neutron reflux of 2.10 m^{-2}S^{-1}. INAA was applied because of difficulties in dissolving the samples. The method proceeds in three steps, irradiation of the elements with neutrons in the nuclear reactor, followed by a period of decay, and finally a measurement of the radioactivity resulting from irradiation.

Catalytic tests

The liquid phase Friedel-Crafts benzylation reaction over Fe-MCM-41 was carried out in a magnetically stirred round-bottomed flask fitted with a reflux condenser and heated in a temperature-controlled oil bath. In a typical reaction, 0.1 g of catalyst (which had been activated overnight at 180°C) was introduced into the reaction flask and heated for a couple of hours at 120°C in vacuum. The reaction flask was cooled down until the desired reaction temperature (in the range of 40°C to 80°C) was reached. Then, dried N_2 gas was bubbled through the reaction flask to avoid the effect of moisture. After that, 10 ml of benzene (dried over molecular sieves) and 1.0 g of benzyl chloride were added; this moment was considered the t_0 of the reaction. Liquid samples (in total, never more than 10% of the reaction volume) were taken at regular intervals and analyzed by gas chromatography. A Varian Star 3500 with a Sil 5 CB capillary column (50 m length, 0.53 mm inner diameter) was used, applying a helium carrier gas with 5 psi flow pressure. The chromatograph was equipped with a flame ionization detector. The mass balance of the reaction was closed within 3%.

The method suggested by Sheldon et al [17] was applied to study the stability of Fe-MCM-41. The leaching experiment was carried out for the Fe-2 sample by separating the solid catalyst after 1h by filtration, which was carried out at the reaction temperature, using a micro-membrane filter. The filtrate was quickly returned to the original flask allowing the reaction to proceed further. The solid residue was sent to elemental analysis for quantitative evaluation using neutron activation analysis (INAA).

Results and discussion

Structure of the catalysts

Figure 1 depicts XRD patterns of various samples of Fe-MCM-41 as compared with iron oxide (Fe_2O_3) pattern. All Fe-MCM-41 samples showed a single intensive peak at low angle, indicating that Fe-MCM-41 is a meso-structured material. This peak shifted in accordance with the d-spacing of each sample. The peak intensity slightly decreases with the Fe-loading, indicating an influence of iron-loading on the integrity of the mesoporous structure. Additionally no bulk Fe_2O_3 or other phases could be detected in any of the prepared samples.

The elemental analysis and the porosity measurements obtained from N_2 adsorption measurements at 77 K are listed in Table 1. Elemental analysis showed that the Si/Fe ratio obtained after calcination is quite similar to that present in the synthesis gel, which indicates that most of Fe cations are incorporated into the solid final product. All Fe-MCM-41 samples showed type IV adsorption isotherms, indicative for meso-structured character [18]. The pore

structure parameters of Fe-MCM-41 showed that the surface area increases with Fe content, while the pore volume and pore diameter decreased.
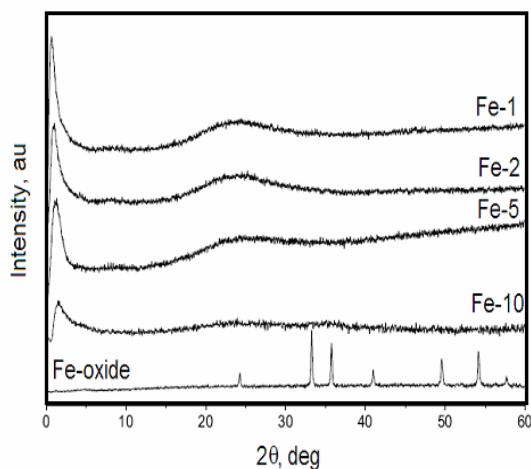

Figure 1. X-ray diffraction patterns of the prepared Fe-MCM-41 samples
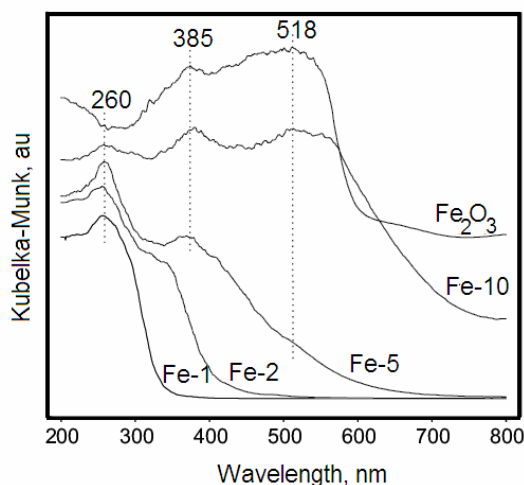
Figure 2. UV-vis spectra for Fe-MCM-41 samples compared with Fe_2O_3.

Table 1. Description for the samples prepared.

Sample	Si/M		Isolated M^{n+}	Nanoparticle M-oxide	Extra-framework M-oxide	S_{BET}[a] m^2/g	V_{meso}[b] Cm^3/g	D_{meso}[c] nm
	Synthesis Mixture	Calcined Product						
Fe-1	100	112	abundant	Absent	Absent	568	1.82	15.9
Fe-2	50	52	abundant	Absent	Absent	625	1.24	11.5
Fe-5	20	18	abundant	Abundant	Absent	803	0.70	5.2
Fe-10	10	10.1	abundant	Abundant	Absent	874	0.45	3.7
Ga-2	50	51	abundant	Absent	Absent	665	0.65	12.7
Sn-2	50	49.6	abundant	Absent	Absent	684	1.03	11.6
Ti-2	50	51.3	abundant	Absent	Absent	533	1.50	12.6

[a] Specific surface area, [b] Mesopore volume and [c] Mesopore diameter.

Figure 2 shows the diffuse reflectance UV–Vis spectra of the Fe-MCM-41 samples. All samples exhibit a peak around 260 nm. This band is assigned to the charge transfer between the Fe^{3+} and O^{2-} atoms in the framework of Fe–O–Si, indicating isolated, tetrahedrally-coordinated Fe species[19].

In addition to this peak, a shoulder appeared at around 330 nm in the Fe-2 sample which would be consistent with the presence of polyferrate $(Fe-O-Fe)_n$ in the framework. At still higher Fe content, extra peaks were observed around 385 and 518 nm for the Fe-5 and Fe-10 samples, indicating the presence of either extra-framework iron or iron oxide particles at high Fe content[20].

Effect of metal loading

Table 2 shows the results of the Friedel-Craft's benzylation of benzene at 60^oC over several calcined Fe-MCM-41 mesoporous samples. Siliceous MCM-41 and Fe_2O_3 were tested as

reference materials. It is clear that siliceous MCM-41 does not catalyze the reaction at all and no products were detected. When bulk Fe_2O_3 was used as a catalyst, only a small conversion was achieved after 4 hours which gave an indication that the dispersed Fe^{3+} containing mesoporous MCM-41 matrix is essential to catalyze this reaction.

Table 2. Conversion of benzyl chloride at $60^{o}C$ over different Fe-MCM-41 samples compared with blank siliceous MCM-41 and Fe_2O_3.

Sample	Si/M	Conversion, %	Reaction time, min.
MCM-41	∞	0	240
Fe_2O_3	0	5	240
Fe-1	113	86	240
Fe-2	54	92	180
Fe-5	21	89	10
Fe-10	10	90	< 1.5
Ga-2	51	65	240
Sn-2	50	16	240
Ti-2	51	4	240

Reaction kinetics

The rate data (time-dependent benzyl chloride conversion data) for the benzene benzylation reaction (with excess of benzene) over the Fe-MCM-41 catalysts could be fitted well to a pseudo-first-order rate law,

$$\ln\left[\frac{1}{1-x}\right] = k(t - t_0)$$

Where k is the first-order rate constant, x is the fractional conversion of benzyl chloride, t is the reaction time and t_0 is the induction period, corresponding to the time required for reaching the equilibrium temperature. A plot of log (1/1-x) as a function of time gave a linear plot over a large range of benzyl chloride conversions (Figure 3). These results are in agreement with the results reported elsewhere [21].

In Figure 4, the rate constants were plotted against the concentration of Fe in the 4 samples of Fe-MCM-41, the relationship showed non-linear behaviour as indication for the change in the nature of the active sites.

Effect of temperature and calculation of activation energy (Ea)

To study the effect of temperature on the reaction rate, reactions were carried out at three different temperatures per sample. Figure 5 depicts the conversion of benzyl chloride over different Fe-MCM-41 samples at different temperatures. It is clear that the catalytic performance is strongly improved by increasing the reaction temperature. The rate constants at different temperatures for the different Fe-MCM-41 samples are listed in Table 3.
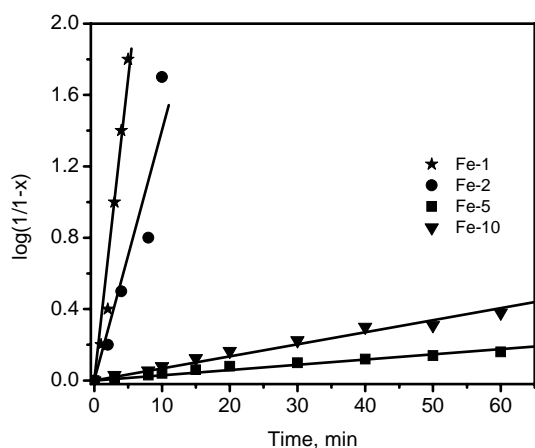
Figure 3. Pseudo 1st order plots for the benzylation of benzene over different Fe-MCM-41 samples at 60°C.
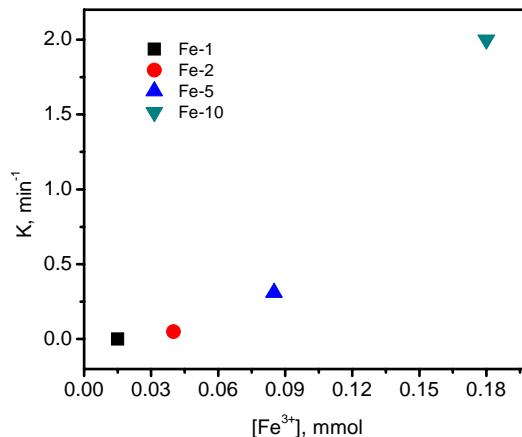
Figure 4. The non-linear behaviour of different Fe-MCM-41 samples in catalytic activity, obtained by plotting the reaction rate constants as a function of active Fe sites.
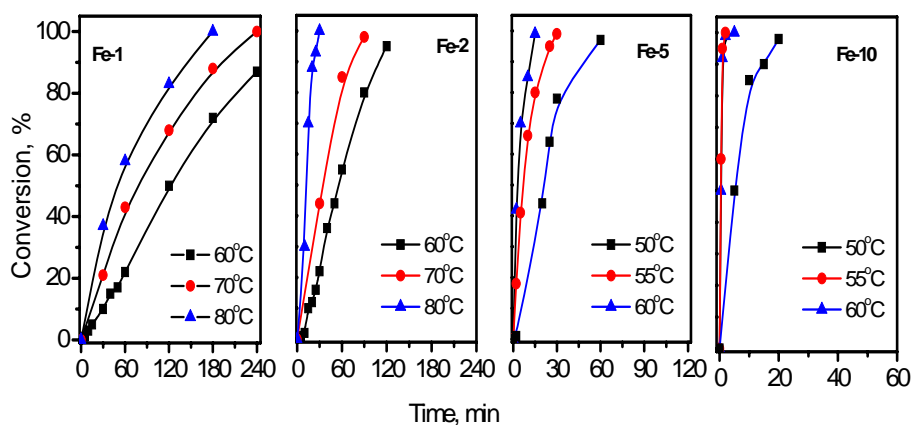

Figure 5. The conversion of benzyl chloride over Fe-MCM-41 samples at different temperatures.

The activation energy was calculated from the Arrhenius equation:

$$K = A \exp^{\frac{-Ea}{RT}}$$

From the above equation at two different temperatures follows:

$$\ln \frac{K_1}{K_2} = \frac{E_a}{R}\left[\frac{1}{T_2} - \frac{1}{T_1}\right]$$

where *A* is the frequency factor (min⁻¹), *Ea* is the activation energy (kJ mol⁻¹), *R* is the universal gas constant (8.314 J.mol⁻¹ K⁻¹) and *T* is the reaction temperature (*K*).
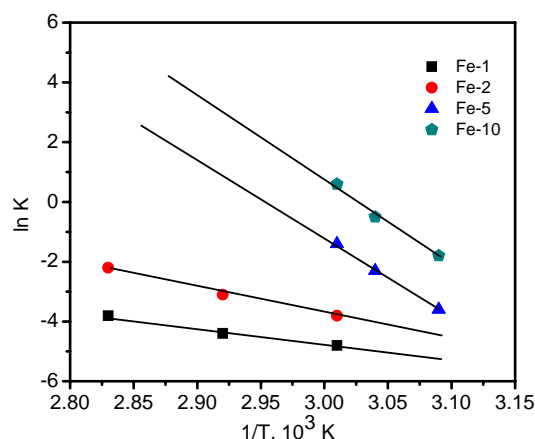
Figure 6. Arrhenius plot for pseudo1st order rate constants.

Table 3. Kinetic parameters for he benzylation of benzene over different Fe-MCM-41 samples.

Sample	First order rate constant K (10^3 min^{-1+})					Activation Energy KJ.mol^{-1}
	323	328	333	343	353	
Fe-1	-	-	9	12	24	47
Fe-2	-	-	22	45	120	85
Fe-5	40	100	310	-	-	182
Fe-10	194	601	2167	-	-	216

The large difference in the activation energy of the Fe-1 and Fe-2 samples *vs.* the Fe-5 and Fe-10 samples might be explained by different kinetically rate determining steps, related to the presence of the nano-particles of Fe-oxide present in the catalysts. This will be further evaluated in the following paragraphs.

Reaction mechanism

The redox properties play an important role in the reaction mechanism of benzene benzylation [9]. It has been proposed that the reaction can be initiated by an oxidation of benzyl chloride over isolated Fe^{3+} with the formation of carbocations (equation 2) after radical formation was initiated in solution (equation 1); the carbocations can attack the aromatic substrate directly without activation (equation 3), as a normal electrophilic substitution reaction, to form the benzylated product. The reaction mechanism over Fe-1 and Fe-2 can be described as:

$$C_6H_5\!-\!CH_2Cl + Fe^{3+} \longrightarrow C_6H_5\!-\!CH_2^{\bullet+} + Cl^{\bullet} \qquad (1)$$

$$C_6H_5\!-\!CH_2^{\bullet+} \longrightarrow C_6H_5\!-\!CH_2^{+} + Fe^{2+} \qquad (2)$$

$$C_6H_5\!-\!CH_2^{+} + C_6H_5\!-\!H \longrightarrow C_6H_5\!-\!CH_2\!-\!C_6H_5 \qquad (3)$$

$$Fe^{2+} + {}^{\bullet}Cl \longrightarrow Fe^{3+} + Cl^{-} \qquad (4)$$
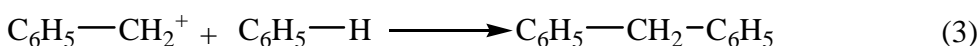
Reaction (3), the electrophilic substitution of benzene, is the proposed rate determining step. The energy difference of 38 kJ/mol between Fe-1 and Fe-2 samples is as yet not well understood, most probably it is due to experimental errors. Significantly still higher activation energy was observed for the Fe-5 and Fe-10 samples. To explain the latter, it can be

hypothesized that the activation of benzene is catalysed by the nano-particles of Fe-oxide as follows:

$$C_6H_5\!-\!H + -\!Fe\!-\!O \rightleftharpoons \overset{\delta-}{C_6H_5}\cdots\overset{\delta+}{H} \;\cdots Fe\cdots O- \tag{5}$$

This step (proposed earlier in [22]) facilitates the reaction between the benzyl carbocation obtained in (2) and the activated benzene. Reaction (3) is now represented by reaction (6).

$$C_6H_5\text{--}H + C_6H_5\!-\!CH_2^+ \longrightarrow C_6H_5\!-\!CH_2\!-\!C_6H_5 + H^+ \tag{6}$$
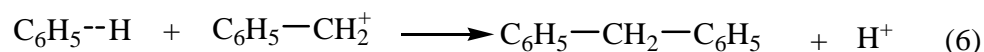
It is clear that step (6) is much faster than the normal electrophilic substitution step (3). In view of the high activation energy, it can be hypothesized that now reaction (1) becomes rate determining. The proposed mechanism is schematically illustrated in Figure 11. It is important to mention that for the newly proposed mechanism to be viable, the isolated sites and the nano-particles have to be located in close proximity. This is very likely to be the case in the MCM-41 catalysts, since the characterization results indicate that the nanoparticles are located inside the mesopores of MCM-41, whereas most of the isolated Fe^{3+} sites are incorporated in the surface of the pores of MCM-41[23].
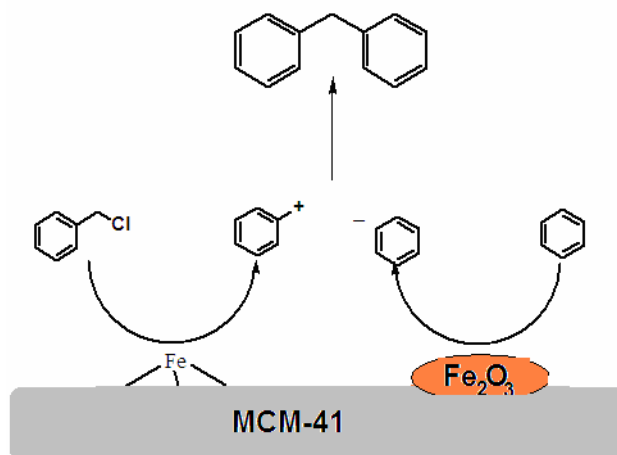

Figure 7. Scheme of benzene benzylation catalyzed by Fe-MCM-41. The Fe^{3+} isolated sites activate the benzyl chloride and the Fe_2O_3 nano-particles activate the benzene ring. The two intermediates react relatively fast.

Actually, the calculated activation energies are remarkable. Experimentally, the results obtained form the two sets of the reaction, which that were controlled by GC are trustable. However, the fact that the kinetic data set is very limited and hence the reported activation energies have to be interpreted with caution. An argument in favor for the two sets of activation energies, is that the high activation energy was obtained for catalysts that clearly contain a significant amount of iron oxide nano-particles, whereas the lower activation energy was related to the catalysts which contain only isolated iron sites. Moreover, the calculated pre-exponential factor for Fe-10 is significantly larger (250 times higher) than Fe-1. Hence the presence of two different reaction mechanisms is, most likely, the suitable explanation.

Stability of Fe in MCM-41 framework

A leaching experiment showed that after separating the catalyst by hot-filtration, the reaction did not continue, the amount of benzyl chloride remaining constant (Figure12). However, elemental analysis showed that almost 33% of the Fe atoms have been removed from the framework (before Si/Fe ratio = 64, and after = 98). This strongly suggests that the reaction proceeded heterogeneously and although Fe was leached, this did not initiate further conversion. Thus, Fe-MCM-41 catalysts represent category (II) of Sheldons' leaching classification [24], i.e. metal is leaching from the framework, but it does not catalyze the reaction.
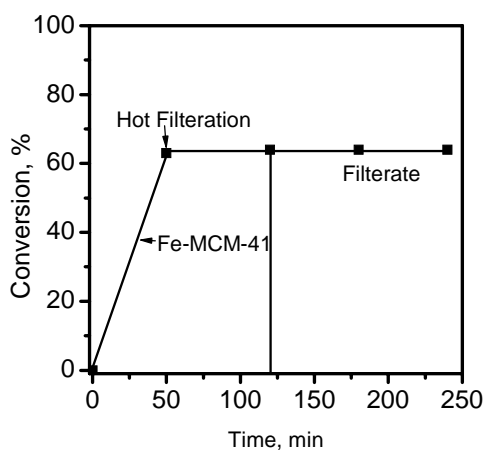

Figure 8. Leaching experiment for benzyl chloride over Fe-2, the catalyst has been hot-filtrated off after 1 hour.

Comparison between Fe-MCM-41 and other catalysts

A comparison between the activity of Fe-MCM-41 with the activities of other mesoporous and microporous materials -as previously reported- is presented in Figure 13, the reactions were carried out in comparable conditions*.
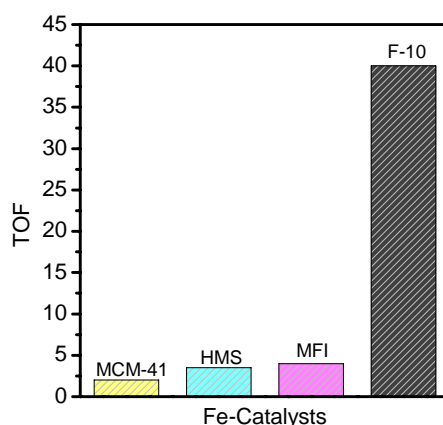

Figure 9. Comparison between the catalytic activity (TOF) over different meso- and microporous catalysts reported as Fe-MCM-41 [14], Fe-HMS [12,22] and Fe-MFI[12] with Fe-MCM-41 (Fe-10 sample).

The comparison showed that Fe-MCM-41 (whatever the loading is) was more active than other Fe-containing microporous materials. This can be attributed to the mesoporous structure

of the catalysts which allows higher accessibility of the substrates. Wider pores which allow the easy movement of the substrate molecules towards the active sites and the simultaneous presence of iron oxide nano-particles as well as isolated iron species are unique for the MCM-41 matrix.

Conclusions

From the present study of the Friedel-Crafts' benzylation of benzene over M-MCM-41 (M = Fe, Ga, Sn and Ti), the following conclusions can be drawn:

1- Fe-MCM-41 was the most active catalyst compared to other M-MCM-41 catalysts, due to the higher redox potential of Fe^{3+} incorporated in the MCM-41 silica matrix.

2- In general, the Fe-MCM-41 samples with Fe_2O_3 nano-particles show very high activity, i.e. 100% conversion within 90-600 seconds. Based on a kinetic study, a synergy of two different active sites (Fe^{3+} and Fe_2O_3 nanoparticles) might explain the high activity.

3- Fe-MCM-41 with a wide pore system, allows high substrate accessibility, explaining the excellent performance compared to other Fe systems, such as Fe-HMS or Fe-ZSM-5.

References.
1- G.A. Olah, in "*Friedel-Crafts and related reactions.*" Wiley-Interscience, New York, 1963; Vol. 1, Chap. 1.
2- J.H. Clark, S.R. Cullen, S.J. Barlow and T.W. Bastock, *J. Chem. Soc., Perkin Trans., 2*, 1117 (1994).
3- J.H. Clark, A.P. Kybett, D.J. Macquarrie, S.J. Barlow and P. Landon, *J. Chem. Soc., Chem. Commun.*, 1353 (1989).
4- M. Campanati, F. Fazzini, G. Fornasari, A. Tagliani, A. Vaccari and O. Piccolo, *Chem. Ind.*, 307 (1998).
5- T. Cseri, S. Bekassy, F. Figueras and S. Rizner, *J. Mol. Catal. A* **98**, 101 (1995).
6- B. Choudary, M. Kantam, M. Sateesh, K. Rao and P. Santhi, *Appl. Catal. A* **149**, 257 (1997).
7- E. Rightor, M. Tzou and T. Pinnavaia, *J. Catal.* **130**, 29 (1991).
8- I. Yusuke, O. Mayumi and U. Kazuo, *Appl. Catal. A* **132**, 127 (1995).
9- I. Yusuke, O. Mayumi, N. Wataru and U. Kazuo, *Chem. Lett.* **10**, 1987 (1992).
10- B. Coq, V. Gourves and F. Figueras, *Appl. Catal. A* **100**, 69 (1993).
11- A. Singh and D. Bhattacharya, *Catal. Lett.*, 327 (1995).
12- V.R. Choudhary, S.K. Jana and B.P. Kiran, *Catal. Today* **59**, 217 (1999).
13- J. Cao, N. He, C. Li, J. Dong and Q. Xu, *Stud. Surf. Sci. Catal.* **117**, 461 (1998).
14- N. He, S. Bao and Q. Xu, *Appl. Catal. A* **169**, 29 (1998).
15- W. Stöber, A. Fink and E.J. Bohn, J. Colloid Interface Sci., **26**, 62 (1968).
16- F. Boynton, "*Neutron activation analysis*" in *Handbook on the Physics and Chemistry;* K. Gschneidner, J., L. Eyring.(Eds). Holland Publishing Company, Amsterdam, 1979; pp 457-470 (Chapter 37F).
17- R.A. Sheldon, I.W. Arends and H.E. Lempers, *Catal. Today* **41**, 387 (1998).
18- K. Sing, D. Everett, R. Haul, L. Moscou, R. Pierotti, J. Rouquerol and T. Siemieniewska, *Pure Appl. Chem.* **57**, 603 (1985).
19- B. Echchahed, A. Moen, D. Nicholson and L. Bonneviot, *Chem. Mater.,* **9**, 1716 (1997).
20- Y. Wang, Q. Zhang, T. Shishido and K. Takehira, *J. Catal.* **209**, 186 (2002).
21- K. Bachari, J. Millet, B. Benaichouba, O. Cherifi and F. Figueras, *J. Catal.* **221**, 55 (2004).
22- V.R. Choudhary and S.K. Jana, *Appl. Catal. A* **224**, 51 (2002).
23- Z. Shan, J.C. Jansen, L. Marchese and T. Maschmeyer, *Microporous Mesoporous Mater.* **48**, 181 (2001).
24- I.W. Arends and R.A. Sheldon, *Appl. Catal. A* **212**, 175 (2001).